Journal of Hydrology 560 (2018) 160–172

Contents lists available at ScienceDirect

Journal of Hydrology

journal homepage: www.elsevier.com/locate/jhydrol

Research papers

Multi-timescale sediment responses across a human impacted river-estuary system

Yining Chen [a,b], Nengwang Chen [a,*], Yan Li [a,b], Huasheng Hong [a]

[a] Fujian Provincial Key Laboratory for Coastal Ecology and Environmental Studies, Key Laboratory of the Coastal and Wetland Ecosystems, College of the Environment and Ecology, Xiamen University, Xiamen 361102, China

[b] Second Institute of Oceanography, SOA, Hangzhou 310012, China

ARTICLE INFO

Article history:
Received 3 December 2017
Received in revised form 26 February 2018
Accepted 27 February 2018
Available online 2 March 2018
This manuscript was handled by G. Syme, Editor-in-Chief

Keywords:
Suspended sediment
Mountainous river
Estuary
Dam construction
Jiulong River

ABSTRACT

Hydrological processes regulating sediment transport from land to sea have been widely studied. However, anthropogenic factors controlling the river flow-sediment regime and subsequent response of the estuary are still poorly understood. Here we conducted a multi-timescale analysis on flow and sediment discharges during the period 1967–2014 for the two tributaries of the Jiulong River in Southeast China. The long-term flow-sediment relationship remained linear in the North River throughout the period, while the linearity showed a remarkable change after 1995 in the West River, largely due to construction of dams and reservoirs in the upland watershed. Over short timescales, rainstorm events caused the changes of suspended sediment concentration (SSC) in the rivers. Regression analysis using synchronous SSC data in a wet season (2009) revealed a delayed response (average 5 days) of the estuary to river input, and a box-model analysis established a quantitative relationship to further describe the response of the estuary to the river sediment input over multiple timescales. The short-term response is determined by both the vertical SSC-salinity changes and the sediment trapping rate in the estuary. However, over the long term, the reduction of riverine sediment yield increased marine sediments trapped into the estuary. The results of this study indicate that human activities (e.g., dams) have substantially altered sediment delivery patterns and river-estuary interactions at multiple timescales.

1. Introduction

Rivers convey a large amount of land-derived sediments to estuaries, adjacent continental shelves and sometimes the deep sea through complicated processes over various timescales (Liu et al., 2008; Milliman et al., 2007; Meade, 1996; Milliman and Syvitski, 1992; Milliman and Meade, 1983). Although there is little doubt about the importance of river sediment delivery to estuaries and coasts, understanding the nature and magnitude of river changes which influence estuaries and the subsequent response, including particularly timescale effects, remain a challenge (Lane et al., 2007; Dearing and Jones, 2003; Walling, 1983).

It is well understood that sediment delivery to the sea by small mountainous rivers differs from large rivers. Mountainous rivers play important roles in the transfer of terrigenous sediment to the global ocean (Milliman and Syvitski, 1992), shaping the short-term and long-term characters of the coast and seafloor (Milliman et al., 2007; Syvitski and Saito, 2007). During a pooling data study on sediment discharges by global rivers to the sea, Milliman and Syvitski (1992) pointed out that the small mountainous rivers in South Asia (including southeast China as classified by these authors) and Oceania stood out as an exception in comparison to other regions: they generally have very high sediment yields and are sensitive to human disturbance and climate changes. The delivery of suspended sediment to the sea from many of the world's rivers has drastically decreased as a result of human activities over the last decades, particularly the construction of dams and reservoirs, resulting in sediment retention (e.g., Li et al., 2012; Milliman and Farnsworth, 2011; Meade and Moody, 2010; Dai et al., 2009). Due to their small size and generally steep gradient, small rivers in the South Asia are also more sensitive to human activities and episodic events (e.g., rainstorms and typhoons) (Huang et al., 2013; Milliman et al., 2007; Kao et al., 2005; Milliman and Kao, 2005; Syvitski et al., 2005; Lin et al., 2002).

River sediment flux to the sea has been estimated by a variety of studies, mainly based on gauging stations data (Dai et al., 2008; Walling and Fang, 2003; Milliman and Syvitski, 1992; Meybeck, 1988). In order to improve the precision of estimates, the linkage between the river input at gauging stations and the estuary output

* Corresponding author.
E-mail address: nwchen@xmu.edu.cn (N. Chen).

https://doi.org/10.1016/j.jhydrol.2018.02.075

should be established. Some models have been used to estimate the suspended sediment transported from tributaries passing dams over a short time period (Wall et al., 2008; David et al., 2006), but further improvements are required to include the effects of tidal transport at the estuary at multiple timescales. A small mountainous river and its estuary form a simple system for such a conceptual model to be established.

The main purposes of our study are: (1) to identify primary factors influencing the flow and sediment discharges of a small mountainous river under intense human impacts; and (2) to establish the relationship between the river input and estuary output over multiple timescales, based on river-estuarine synchronous data and box model analysis.

As the second largest river in Fujian Province of China, the Jiulong River's annual sediment yield averages about 2.5 Mt. This is a typical mountainous river in Southeast China, with a catchment basin greatly affected by various human activities, such as hydropower station construction and land use changes. In addition, the estuary of the Jiulong River is dominated by macro-tides. Therefore, the significant river inputs encounter a strong tidal force within the estuary, resulting in a complex process of mass (water and sediments) exchange. The riverine inputs under intensive human impacts, together with the significant tidal force into the estuary, provides an ideal case to study the linkage between riverine input and estuary response.

This paper is arranged as follows: (1) analyses of flow discharge and sediment discharge data of Jiulong River between 1967 and 2014, in order to understand the short-term (episodic), medium-term (seasonal), and long-term (~50 years) river input changes, and their controlling factors; (2) understand the linkages between river input and estuary response over a wet season; (3) Supplementary cruise survey data to provide the basis for model analysis; and (4) box model analysis to establish the relationship between river input and estuary output over multiple timescales.

2. Materials and methods

2.1. Description of study area

The area under investigation is the Jiulong River and its estuary, located on the western side of the Taiwan Strait, Southeast China (Fig. 1). The watershed includes two major river reaches, namely the North River and West River. The North River covers a watershed area of 9640 km^2, with a total length of 297 km and an average elevation of 613 m. The West River watershed area covers 3940 km^2, with a total length of 172 km and an average elevation of 402 m (Zhang et al., 2015). Annual precipitation averages 1400–1800 mm, of which 70% occurs between April and September. This region is also affected by intense typhoon occurrence (1.35 per year), mainly between July and September (Xu and Hong, 2000). The soil erosion modulus of the catchment in 2002 was estimated to be 2730 tons km^{-2} yr^{-1} (Huang et al., 2004), and total soil erosion decreased 5% from 1989 to 2003 due to land use changes (Jiang et al., 2007).

The Jiulong River is an important source of hydroelectricity for the watershed. More than 100 hydropower stations on the river were constructed, mostly after 1995, although this number increases remarkably if small hydropower stations in remote tributaries are also included (Wang et al., 2010; Zhu, 2008). There are six major dam reservoirs (primarily for hydropower generation and flood control) in the main stem of the North River, while in the West River, most dams (which are relatively small) are located in tributaries rather than in the main stem. It has been noted that the dam density of the West River is 1.35 times that of the North River, with a large number of small dams constructed after 1995 (Zhang et al., 2015). Human activities, especially cascade hydropower development (Fig. 1), contributed more to the streamflow regime in the Jiulong River watershed than climate changes (Zhang et al., 2015). In addition, the management of large reservoirs differs from that of small dams in terms of flushing operations. Large reservoirs serve as flood controls during the wet season and the sediments trapped within those reservoirs are flushed out during flooding events. In contrast, the operation of small reservoirs in the West River is hardly conducted for economic reasons (personal communication with Jiulong River Reservoir Management Office).

The Jiulong River Estuary (Fig. 1) has a number of islands located on its seaward side, which provide shelter from oceanic wave activity. The water depth within the estuary is generally <15 m (at lowest low water datum), with extensive intertidal mudflats within the main channel and along the coastline. The winds are mainly from the NE and NNE and contribute to the generation of local waves with a maximum significant wave height of 1.8 m (Lin et al., 2009). The mean tidal range is 3.9 m with a maximum range of 6.4 m (Ji, 2006; Jiang and Wai, 2005). From the upper reach to Haimen, water circulation is mainly dominated by river inflow whilst the outside of Jiyu Island is controlled by tides (Wang, 2013). Suspended sediment in the lower estuary shows a main pathway to the south side of the main channel whilst the tidal water enters from the north side. Two high turbidity zones have been observed this estuary: one is located to the west of Haimen Island and the other to the west of Jiyu Island (Wang et al., 2005; Cai et al., 1999).

2.2. Data collection and data processing

This study employs three types of data: long-term daily river flow discharge and sediment discharge data obtained from two gauging stations from 1967 to 2014, medium-term suspended sediment concentration data from a buoy turbidity sensor covering the wet season in 2009, and short-term cruise survey data between 2008 and 2010.

Long-term data include daily flow discharge (m^3 s^{-1}) and daily suspended sediment discharge (or sediment flux, kg s^{-1}) over a 47-year period (1967–2014) from two gauging stations, named Punan Hydrological Station and Zhengdian Hydrological Station. Punan Hydrological Station is located in the downstream of the North River where the drainage area is 8490 km^2, and Zhengdian Hydrological Station is situated in the downstream of the West River where the drainage area is 3419 km^2; these two stations therefore account for more than 80% of the total watershed area of the Jiulong River.

Flow discharge and suspended sediment discharge were measured according to the Chinese national standard criteria. All discharge data were estimated at the same gauging cross-section, within the errors of ±2.5% (flow discharge) and ±3.0% (suspended sediment discharge). The flow discharge was estimated by a combination of flow profile data and water level data. Water samples were taken from a consistent gauging section across the full water column. Suspended sediment concentration was determined gravimetrically as the difference between the pre-weighed and filtered after oven-drying to constant weight.

The sediment discharge is calculated by the mass passing a certain gauging section over a unit time, as the following equation:

$$Q_s = \sum_{n}^{i=1} Q_{w(i)} \times C_{(i)} \quad (1)$$

where Q_s (kg s^{-1}) is sediment discharge, $Q_{w(i)}$ is flow discharge (m^3 s^{-1}) and $C_{(i)}$ is the suspended sediment concentration (mg L^{-1}) at a depth interval (i). The monthly, seasonal and annual data of sus-

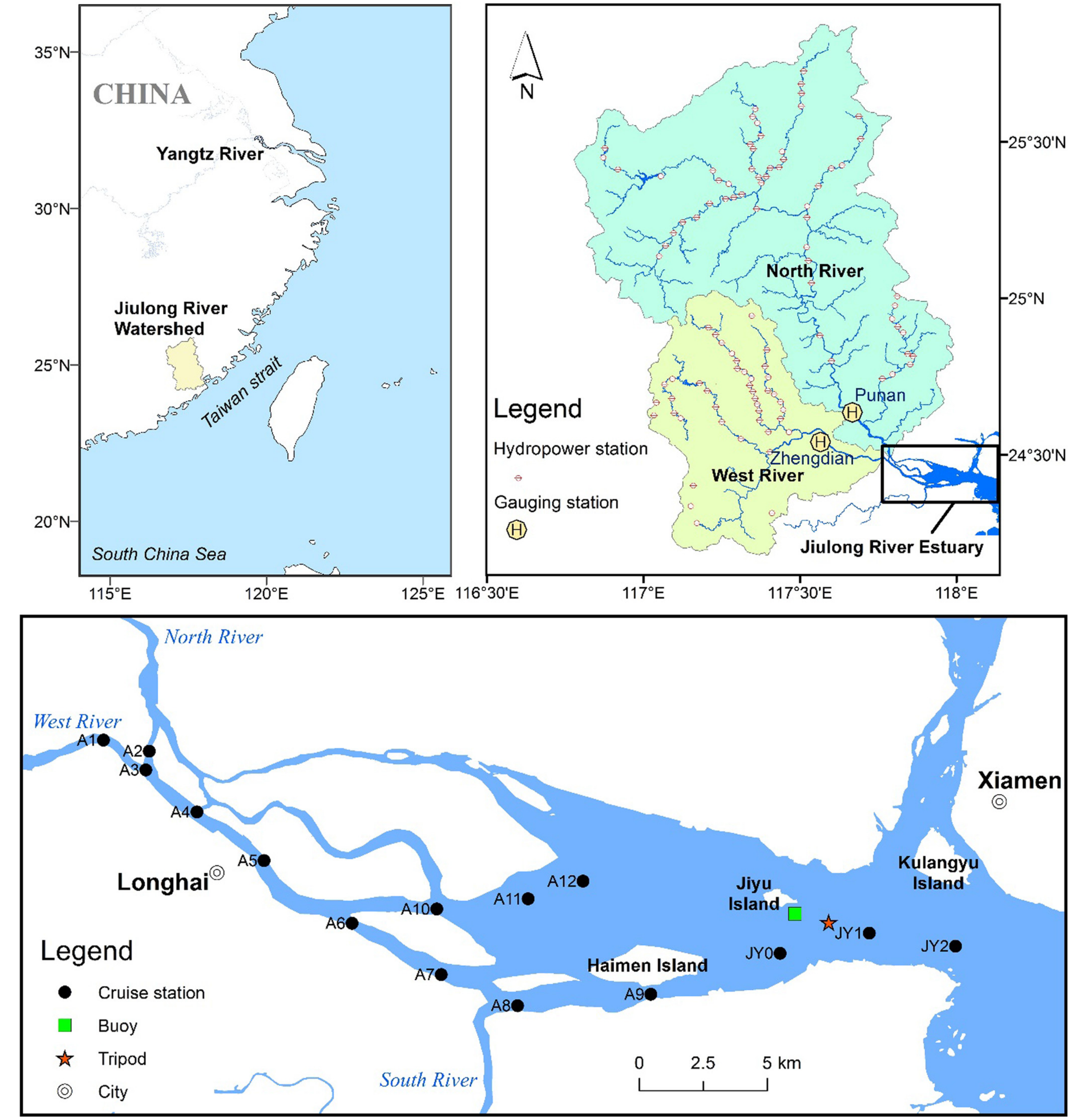

Fig. 1. The map of the site under investigation: the left upper panel illustrates the location of the Jiulong River along Southeast coasts of China; the right upper panel covers the overall Jiulong River watershed and the lower panel provide the details of Jiulong River Estuary. The locations of hydropower stations are based on Zhang et al. (2015). Cruise stations are marked by black dots; the green square indicates the location of the buoy close to Jiyu Island; the red star indicates the location of Tripod which was mounted by Wang et al. (2013) to observe flows and suspended sediments, is also shown in the lower panel.

pended sediment discharge and flow discharge were averaged from these daily data, and the uncertainty was measured by standard deviation of the monthly, seasonal and annual data over the measurement period. Wet season is defined as the period between April and September with the remaining months counted as dry season. The monthly data for flow discharge and sediment discharge are summed throughout the two periods to estimate the proportion of wet and dry seasons. Flow discharge and sediment discharge of the two gauging stations over a wet season in 2009 were converted into SSC (sediment discharge divided by flow discharge) to allow for a comparison with buoy data.

A buoy equipped with a turbidity sensor was released close to Jiyu Island by Xiamen Oceans and Fisheries Bureau and operated between 17th April and 26th September 2009 (Fig. 1). SSC data at hourly intervals were provided by the Oceans and Fisheries Bureau, after calibrating the turbidity data using surface water samples ($SSC = 9.4857 * turbidity$, $R^2 = 0.95$). A low-pass filter was created by a Matlab software package to remove the tidal cycle signal at Jiyu Island, and the time series data were subsequently averaged into daily values as the tidal-filtered SSC of the estuary.

Five cruise surveys were conducted to cover a series of stations from the river above Longhai, downstream along a river-estuary transect (Fig. 1) in August and November 2008, May and late June 2009 and early July 2010. On-board water samples were collected using 5 L Niskin bottles (model QCCC-5, National Ocean Technology Center, China) at each station from the surface (~0.1 H, H = water depth) and the bottom (~0.9 H) for SSC measurement. SSC was measured by passing a known sample volume through a pre-weighed 0.45 μm glass fiber filter, followed by drying and weighing (Tucker, 1988). During the cruise in July 2010, water samples were immediately transported back to the laboratory to analyze the grain size using a laser Malvern Mastersizer 2000 granulometer (range 0.02–2000 μm) following a standard procedure (Tucker, 1988). Due to the hot weather and the subsequent rapid algae bloom in the water samples, most of the samples were found not suitable for grain size analysis, thus only part of the grain size data were obtained and used in this study.

A SPSS software package was used for (1) regression analyses of the relationship between annual flow discharge and annual sediment discharge of the North River and the West River between 1967 and 2014; and (2) nonlinear and linear multiple regression analyses to examine the relationship between the river input and estuary output over a wet season in 2009, using the daily SSC data from the North River, West River and Jiyu buoy (after filtering for tides). Null-hypothesis test was adopted and P-value was used to determine the significant level for all tests.

3. Results

3.1. Monthly river flow and sediment discharge

The monthly flow discharge and sediment discharge data are presented in Fig. 2. Overall, both the North River and West River show the characteristics of mountainous rivers, with remarkable periodic changes. Between 1967 and 2014, the average value of monthly flow discharge of the North River (262.9 ± 212.8 $m^3\ s^{-1}$) was more than twice that of the West River (122.2 ± 94.7 $m^3\ s^{-1}$). In contrast, the average values of monthly sediment discharges between 1967 and 2014 were 70.9 ± 119.0 kg s^{-1} and

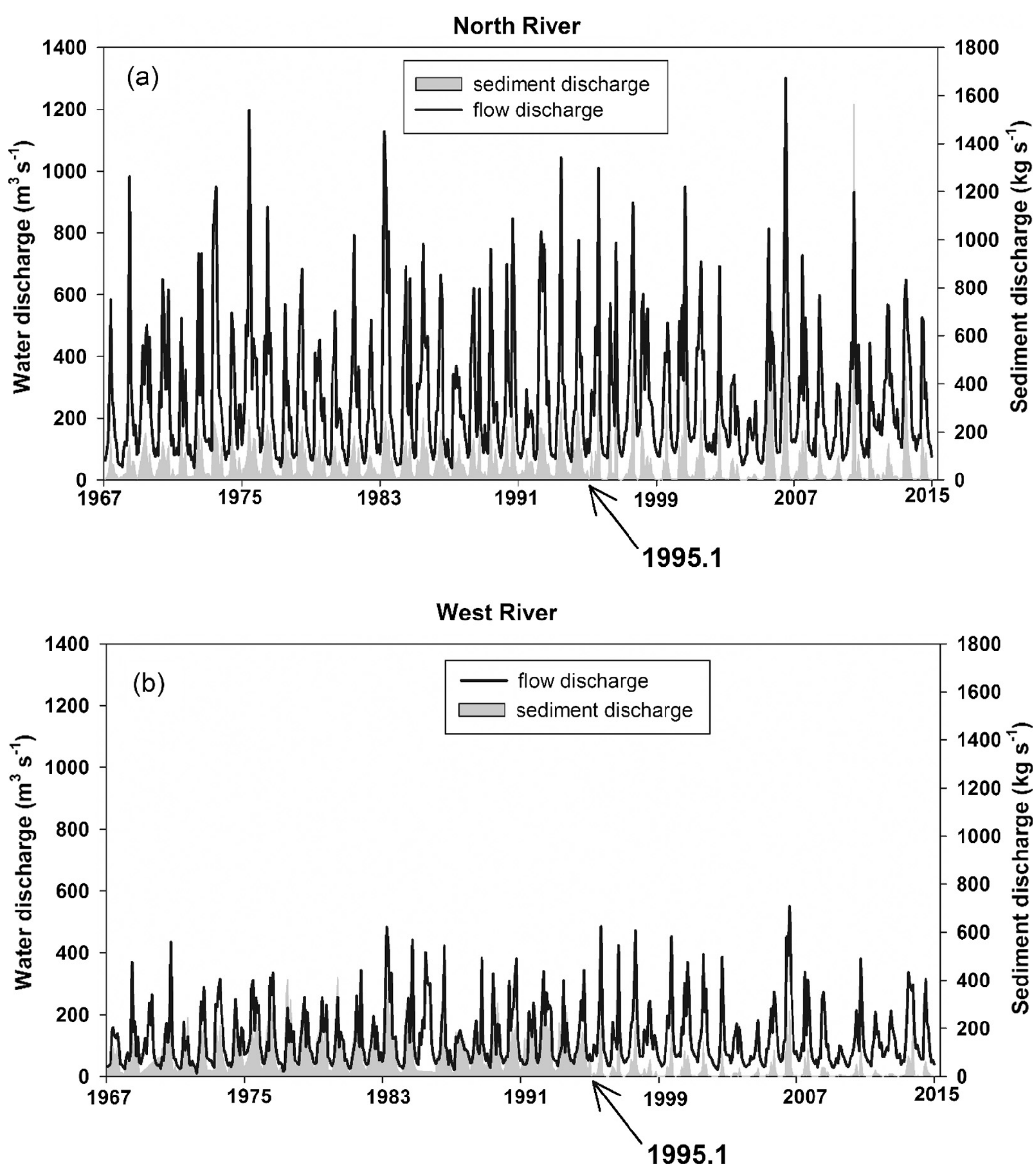

Fig. 2. The monthly data of the flow and the sediment discharges during the period of 1967–2014: (a) North River; and (b) West River.

73.3 ± 83.8 kg s^{-1} for the North River and West River, respectively, so the two rivers contributed almost equally to the sediment discharge from river catchment to coastal water.

There were notable changes in sediment discharge after 1995 both for the North River and West River, as the sediment discharge shifted from a continuous increase to a discontinuous status (Fig. 2). Altogether, the variation in the sediment discharge of the North River shows a total reduction of 11% after 1995, in comparison with the previous average value, but the West River shows a remarkable sediment reduction of 82% on average after this date, despite similar flow discharges from both rivers. These patterns indicate that the behavior of sediment delivery by the two rivers has changed considerably since 1995.

The accumulative curves between flow discharge and sediment discharge is usually used to indicate the turning points of a river system in delivering water and sediment. Fig. 3 illustrates the changes of the two rivers over a period of 47 years based on monthly data. The turning point for the West River can be readily identified to have taken place between 1994 and 1995, and this period is consistent with the pattern of the monthly time series (Fig. 3b). However, the accumulative curve of the North River does not show a clear turning point. After 1995 the curve changes into several segments, and the general trend is only slightly altered.

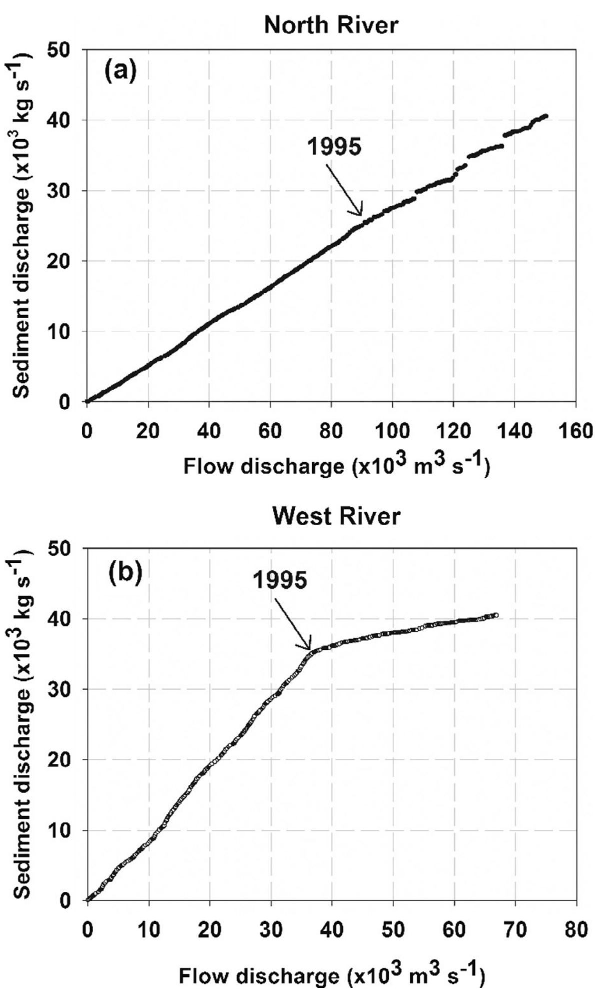

Fig. 3. The accumulative curves of the monthly flow and sediment discharges during 1967–2014: (a) North River; and (b) West River. Turning points are marked with arrows.

3.2. Annual flow and sediment discharge

The annually-averaged flow discharge and sediment discharge data during the study period are displayed in Fig. 4. A remarkable reduction in sediment discharge from the West River can be seen after 1995, whilst the North River demonstrates a greater inter-annual variation after 1995. Before 1995, the North River contributed 8.37×10^9 tons of water and 2.34×10^6 tons of sediment per year whilst the West River delivered 3.83×10^9 tons of water and 3.58×10^6 tons of sediment per year to the estuary. However, after 1995, although the flow discharge of both rivers remained similar, the annual sediment mass delivered by the North River slightly decreased to 2.09×10^6 tons, but there was a much more pronounced reduction in the West River sediment to 6.60×10^5 tons per year. The North River was the primary contributor of fresh water to the estuary throughout the period of observation, whilst the primary contributor of sediment to the estuary changed after 1995 from the West River to the North River.

The relationships between flow discharge and sediment discharge indicate the system behavior features of water and sediment delivery (Fig. 5). A good linear relationship ($R^2 = 0.53$, $P < 0.001$) between flow discharge and sediment discharge can be identified in the North River throughout the period 1967–2014, implying a stable system delivering sediments by river flows in a linear way (Fig. 5a). In contrast, the West River shows a swift in flow-sediment relationship as revealed by the two clustered groups in Fig. 5b. The clustered data between 1967 and 1995 illustrate a much higher ratio between sediment discharge and flow discharge than those of the clustered data between 1995 and 2014. The linear regression of the data 1967–1994 ($R^2 = 0.23$, $P = 0.013$) gives a much lower significance level than the regression after 1995 ($R^2 = 0.80$, $P < 0.001$, Fig. 5b). Considering the significance level of the North River, a significant level of 0.01 is adopt for the null hypothesis test, to differ the linearity of the system.

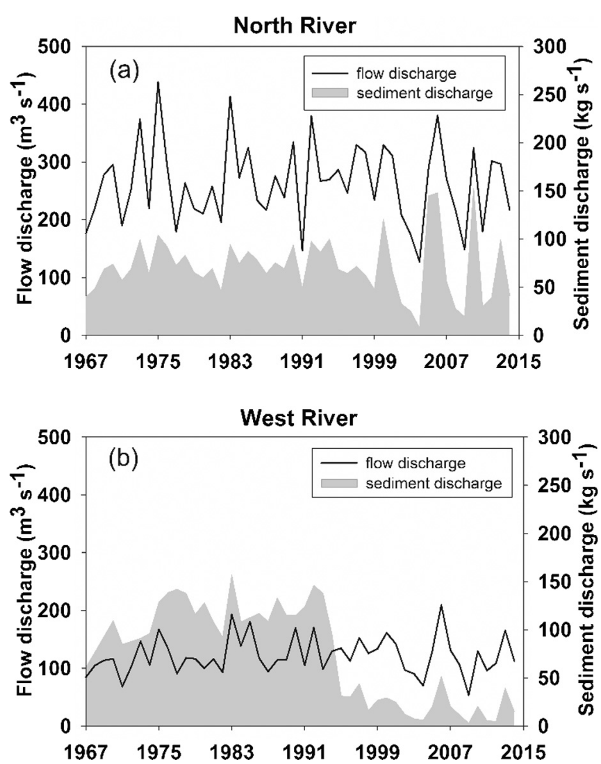

Fig. 4. The annual flow discharge and sediment discharge data over a time span of 1967–2014: (a) the North River; and (b) the West River.

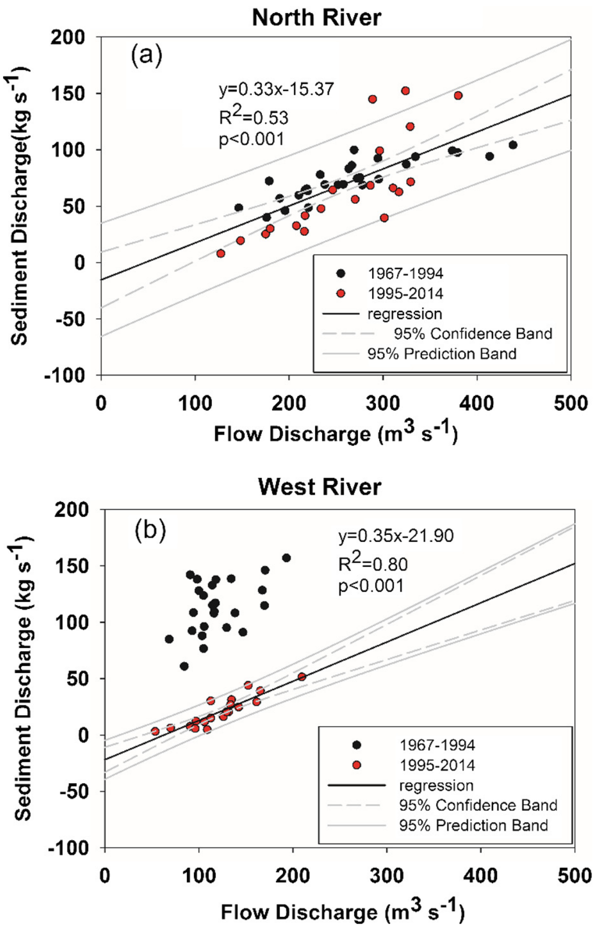

Fig. 5. The relationships between annual flow discharge and sediment discharge: (a) North River; and (b) the West River. The red dots represent the data during 1995–2014 whilst the black dots mark the data during 1967–1994. The regression of the North River data includes all data throughout 1967–2014, whilst the regression of the West River data excludes the data between 1967 and 1994.

Therefore, before 1995, the West River was more like a natural system and the relationship between the flow and sediment transport was more scattered, as in a nonlinear system. Since 1995, however, this river has been altered into a linear system similar to the North River.

3.3. Seasonal patterns in flow and sediment discharges

The seasonal patterns of the North River and West River are displayed in Fig. 6, using mean values and standard deviations from January to December over a period of 47 years. Overall, a wet period with relatively high flow discharge and sediment discharge is observed from both rivers between April and September. Approximately 80% of sediment transport and 73% of flow discharge occurs in the wet season, as calculated by the total wet season amount divided by the total amount of the year. Two peaks, occurring in June and August, correspond to the plum rain season in the early summer and peak typhoon season in the late summer, and this pattern is consistent with previous studies (Huang, 2008).

A comparison of the data for 1967–1994 and 1995–2014 also indicates considerable differences (Fig. 6). Both the flow discharge and sediment discharge of the two rivers during the period 1967–1994 showed a high peak in June, together with a much smoother peak in August. This pattern has changed since 1995, as the flow and sediment discharges now form two nearly equal peaks in June and August.

3.4. The long-transect SSC variation revealed by cruise surveys

There is a considerable variation in SSC and salinity from the upper to lower estuary (Fig. 7). These variations confine the turbidity maximum zone between A6 and A9 (see Fig. 1 for location information). The turbidity maximum zone can be identified by high suspended sediment concentration as pointed out by previous studies (Dyer et al., 2004; Uncles and Stephens, 1993). Although the movement of this zone is associated with various conditions, the range of turbidity maximum zone revealed by this study is consistent with other studies (Wang et al., 2005; Cai et al., 1999). Therefore, it can be inferred that Jiyu Island can be regarded as a transition zone from river-dominance to tidal-dominance (i.e. marking the seaward boundary of the estuary).

Secondly, the cruise SSC data also reveal the changes between top and bottom layers (Fig. 7). Overall, the SSC in the bottom layer is higher than that of the top layer, but with a limited mean range of 20%. The bottom layer SSC of A8 in June 2009 shows an extraordinary high value, and this is probably caused by the occasional presence of fluid muds near the bottom.

The grain size data are also present in Table 1. The suspended sediment particles are mainly clays and silts, as the medium grain size is very low, and the sediments are relatively uniform in terms of constituents between A3 and A9. The particles become slightly coarser due to the increased influence of tides outside of Jiyu Island. A4 and A8 are the only stations to provide a comparison between top and bottom layers, but show a relatively uniform distribution. Overall, the suspended sediments transported from the rivers to the estuary remain relatively stable in terms of constituents and vertical distribution, unless they encounter tidal flows outside Jiyu Island.

3.5. Synchronous SSC data of the gauging stations and estuary over a wet season

The daily data of the Punan, Zhengdian and Jiyu stations are shown in Fig. 8, covering a wet season in 2009. The North River shows an overall high SSC level, with episodic peaks. The significant peaks mainly appeared in June and July, and coincide well with recorded rainstorm events (Fig. 8a). The West River shows a similar pattern to the North River in response to rainstorm events, but with much less magnitude (Fig. 8b). The SSC increase at the hydrological stations generally shows a delay of 1–2 days for both rivers after the rainstorm occurs. Three typhoons occurred during this period, but did not have significant influence on the flow and sediment concentration data of these river sites.

The SSC at Jiyu is in general lower than at the two river sites as shown by Fig. 7. There are no direct links between recorded peaks and rainstorm events, but typhoon events appeared to slightly increase the SSC at the estuary, which might be associated with wave-induced resuspension (Fig. 8c). This pattern implies a more complicated process of sediment transport through the estuary, particularly the turbidity maximum zone. In order to understand the link between the SSC at the river reach and the SSC in the estuary, nonlinear regression analysis on multiple variables was undertaken to statistically test the response of the SSC at Jiyu to the river input. A nonlinear multiple regression model was established (Eq. (2)) at a confidence level of 95%, using the daily SSC data of Jiyu (SSC_j), North River (SSC_n) and West River (SSC_w).

$$SSC_j = 0.42SSC_w - 0.002SSC_w^2 + 0.00007SSC_n^2 - 0.12SSC_n + 54.08 \quad (2)$$

A scale analysis on the sensitivity of each term was further conducted for Eq. (2), using the data during the wet season of 2009. Overall, the mean SSC was 38 mg L^{-1} for the Jiyu station,

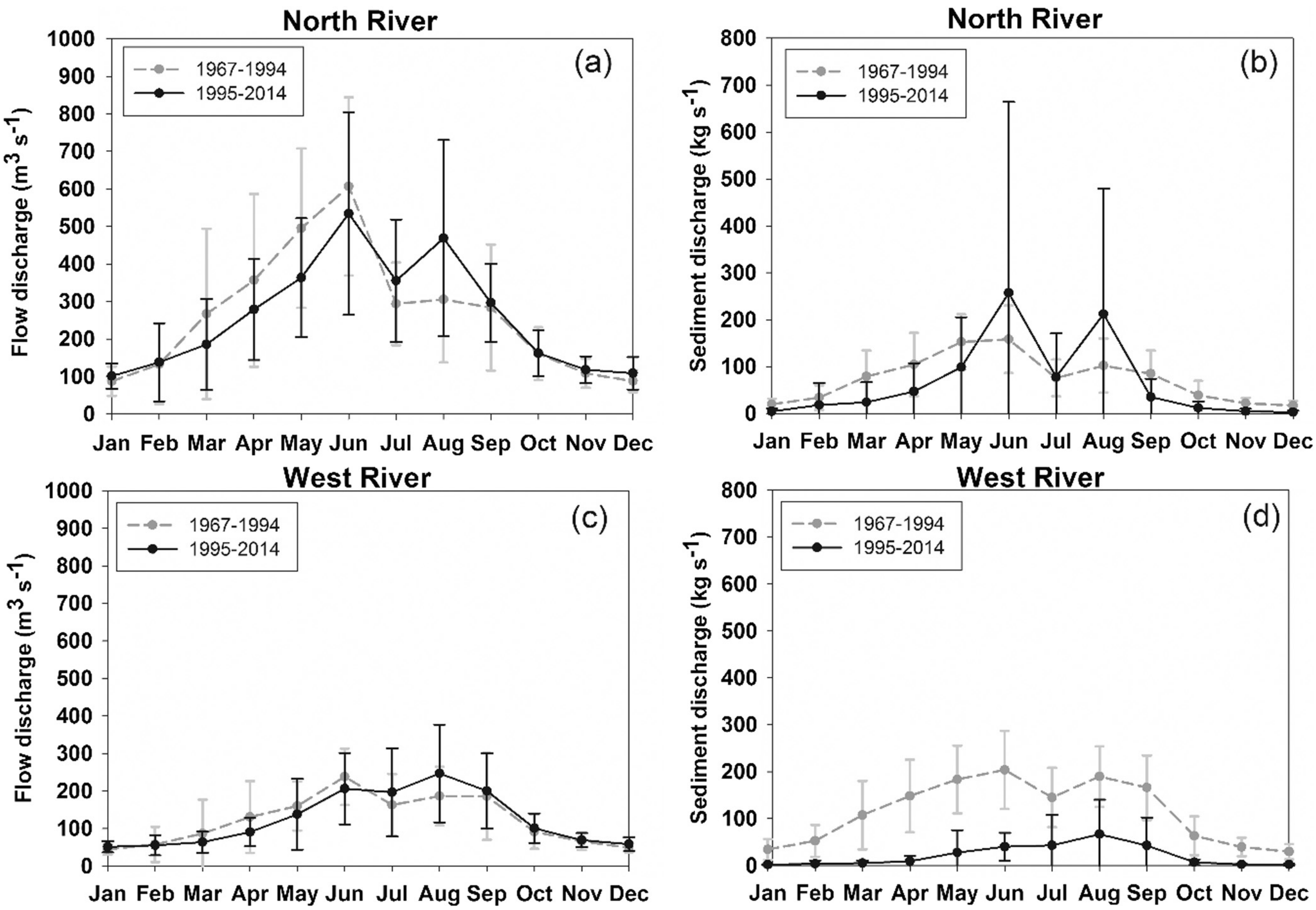

Fig. 6. A comparison in averaged monthly flow discharge and sediment discharge between 1967 and 1994 and 1995–2014: (a) North River, flow discharge; (b) North River, sediment discharge; (c) West River, flow discharge; (b) West River, sediment discharge.

111 mg L^{-1} for the North River and 53 mg L^{-1} for the West River. Therefore, the scale analysis of these terms is shown as Eqs. (3) and (3′).

$$O(10^1) = O(10^{-1} \times 10^1) - O(10^{-3} \times 10^2) + O(10^{-5} \times 10^4) - O(10^{-1} \times 10^2) + O(10^1) \quad (3)$$

$$O(10^1) = O(10^0) - O(10^{-1}) + O(10^{-1}) - O(10^1) + O(10^1) \quad (3')$$

As such, the second and third terms on the right of the equation (the squared terms) can be neglected during this specific period. Only linear terms and the constant remain in the simplified regression model. Therefore, a linear multiple regression model can be used to evaluate the response of the estuary to the river input during the wet season in 2009.

Due to the distance between the hydrological stations and Jiyu Island, a lag in response should be considered in the regression tests, but the time length is unknown. For simplicity, a maximum lag of 10 days was considered for the regression tests and the lowest P-value with relatively high R-value was taken as the criteria for best fit over the 10-day delay (Fig. 9, red circles mark the best fit results).

Both the North River and West River show good linear relationships (P-value < 0.05) with the Jiyu data when the lag is taken into account (Fig. 9a and b). However, a notable difference exists between the suspended sediments from the North and West Rivers: the lag between the North River and Jiyu was found to be 2 days (P-value = 0.035), whilst the lag between the West River and Jiyu was 7 days (P-value = 0.022). It appears that the suspended sediment input from the North River affects the estuary (Jiyu) in a more rapid way (low P-values of the first several days of lag) and then disappears afterwards. In contrast, the estuary responds to the West River input with a longer lag, but with a stronger signal (P-value = 0.022, Fig. 9b).

In order to quantify the individual contribution of the North River and the West River, a multiple regression model was also tested and the results are plotted in Fig. 9c. Given the samples, the multiple regression test rejects the null hypothesis test with a P-value = 0.025 when the lag was 5 days. Therefore, the response of the estuary to the inflow of the North River and West River has an average lag of 5 days. The change of suspended sediment in the river reach required such a time span for the signal to pass the upper reach of the estuary and the turbidity maximum zone, and eventually reached the boundary of the estuary.

4. Discussion

4.1. Primary factors affecting sediment delivery from river to estuary

Numerous factors, including climate, soil erosion and human activities, can affect the river flow and sediment discharge (Woods, 2003; Milliman and Syvitski, 1992). For a small mountainous river, the precipitation and rainstorms associated with climate change, catchment dynamics relevant to sediment yield, and sediment retention due to dams and reservoirs, stand out as sensitive factors, particularly for those controlled by the dry-wet seasonal monsoon climate and episodic weather events. Thus, precipitation,

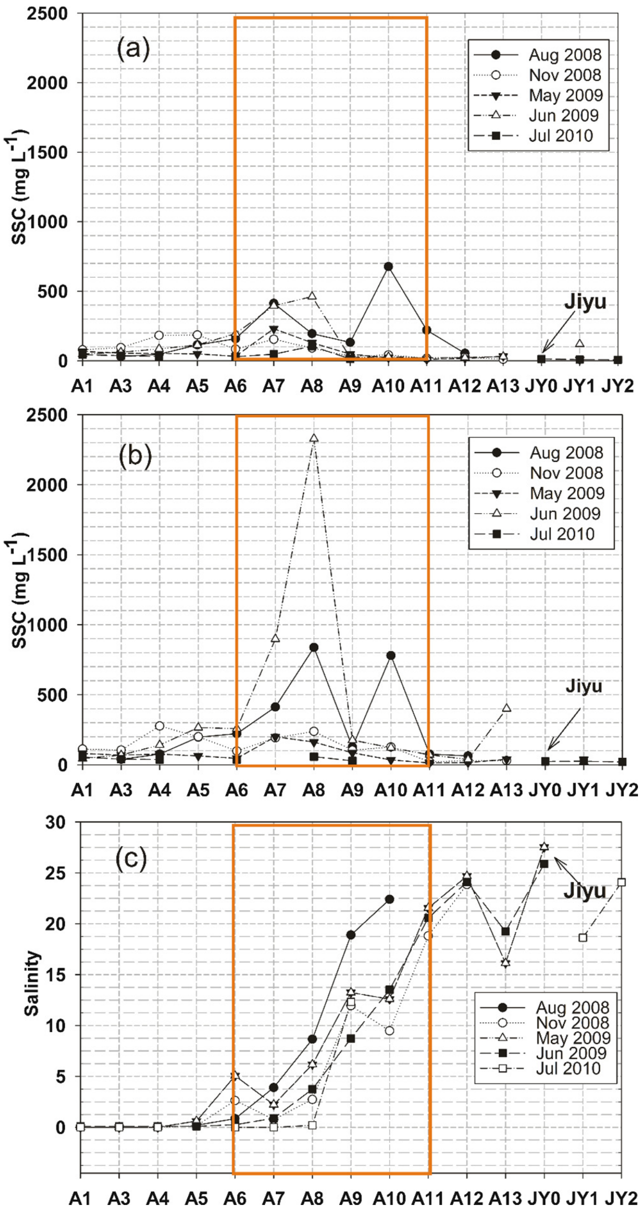

Fig. 7. The spatial variation of SSC and salinity along the river-estuary transect: (a) SSC, top layer; (b) SSC, bottom layer; and (c) salinity. The turbidity maximum usually appears between station A6 and A9 (Fig. 1 for locations), depending on river discharge and tidal conditions during survey periods. The orange box marks the stations with relatively high SSC of the estuary, in coincidence with salinity gradient.

rainstorms, soil erosion and construction of dams and reservoirs are discussed here to extract the most important factors affecting sediment discharge and delivery from Jiulong River, including the 82% reduction in the West River and 11% reduction in the North River after 1995.

Huang et al. (2013) collected precipitation data from the Jiulong River watershed between 1954 and 2010 and discovered a fairly slight increase of precipitation over this period. The annual frequency of rainstorms was found to be correlated with precipitation over a long timescale in their study. A study of stalagmite records reconstructed the precipitation curves and also showed an increase after 1990–1995, together with a considerable change over century scales (Jiang et al., 2012). A more detailed analysis of the rainstorm frequency records between 1971 and 2004 in this region also confirmed a relatively stable pattern of rainstorm frequency (Chen, 2007). Therefore, precipitation and rainstorm frequency related to climate change are less likely to be the main factor for the sediment discharge changes in the Jiulong River over the studied period, but they might be more important over the longer term (centuries). It should also be noted that the precipitation data discussed above include the entire catchment area and there is a possible difference between the North River and West River.

Secondly, land use changes also affect the long-term flow-sediment relationship of rivers (Khoi and Suetsugi, 2012). The Household Contract Responsibility System was formulated in Fujian province in the late 1970s and spread widely during the early 1980s, and this policy greatly stimulated local agricultural production (Ye and Huang, 2009). However, the total area used for agriculture has been shrinking since 1996 because the economic benefits from food crops has decreased (Huang et al., 2012; Ye and Huang, 2009). In addition, the prevention of land erosion by planting grasses or trees commenced by local governments in 1990s, particularly in the catchment of the West River, could also have contributed to the decline of sediment yield (Jiang et al., 2007). Land use change and its influence on sediment yields can be evaluated using soil erosion modulus. Huang et al. (2004) estimated soil erosion to be 2503 tons $km^2\ yr^{-1}$, based on GIS and USLE analyses. A similar method was also adopted in a longer term study from 1989 to 2003, and a decrease of 5% in soil erosion modulus was found during this period (Jiang et al., 2007). It appears that the catchment dynamics related to soil erosion and land use changes only account for a small proportion of sediment discharge reduction over the long term. However, our study shows that over the short-term (within the wet season of 2009), the SSC peaks in the estuary (Jiyu) following the peak at river sites (Punan and Zhengdian). Episodic climate events (rainstorm), particularly continuous rainstorms, show a considerable influence on the sediment transport of this mountainous river. This is because the surface sediment erosion within river catchments is usually caused by overland flow or seepage associated with heavy rainfalls (Garcíaruiz, 2010).

Dams and reservoirs can not only alter the natural streamflow regime by the reduction of peak flow and flood frequency, but also trap the sediments to fill reservoirs (Huang et al., 2013; Takahashi and Nakamura, 2011). The retention in upstream dams can substantially alter the water and suspended sediment transport patterns (Dai et al., 2008; Finger et al., 2006). However, with operation of flushing, most of the fine suspended particles can be flushed out to reach lower streams (Finger et al., 2006). More than 100 hydropower stations have been constructed along the North River and the West River (Wang et al., 2010). In 1994, a series of national government policies were released to encourage the construction of privately-owned small hydropower stations, and a large number of small hydropower dams were constructed along the Jiulong River thereafter; more than 90% of the small

Table 1
The grain size data of water samples collected during the cruise in 2010.

Medium grain size (μm)	A3	A4	A6	A8	A9	JY0	JY1
Top	–	9.0	–	8.5	–	14.3	–
Bottom	9.7	9.4	10.1	10.9	10.7	–	16.1

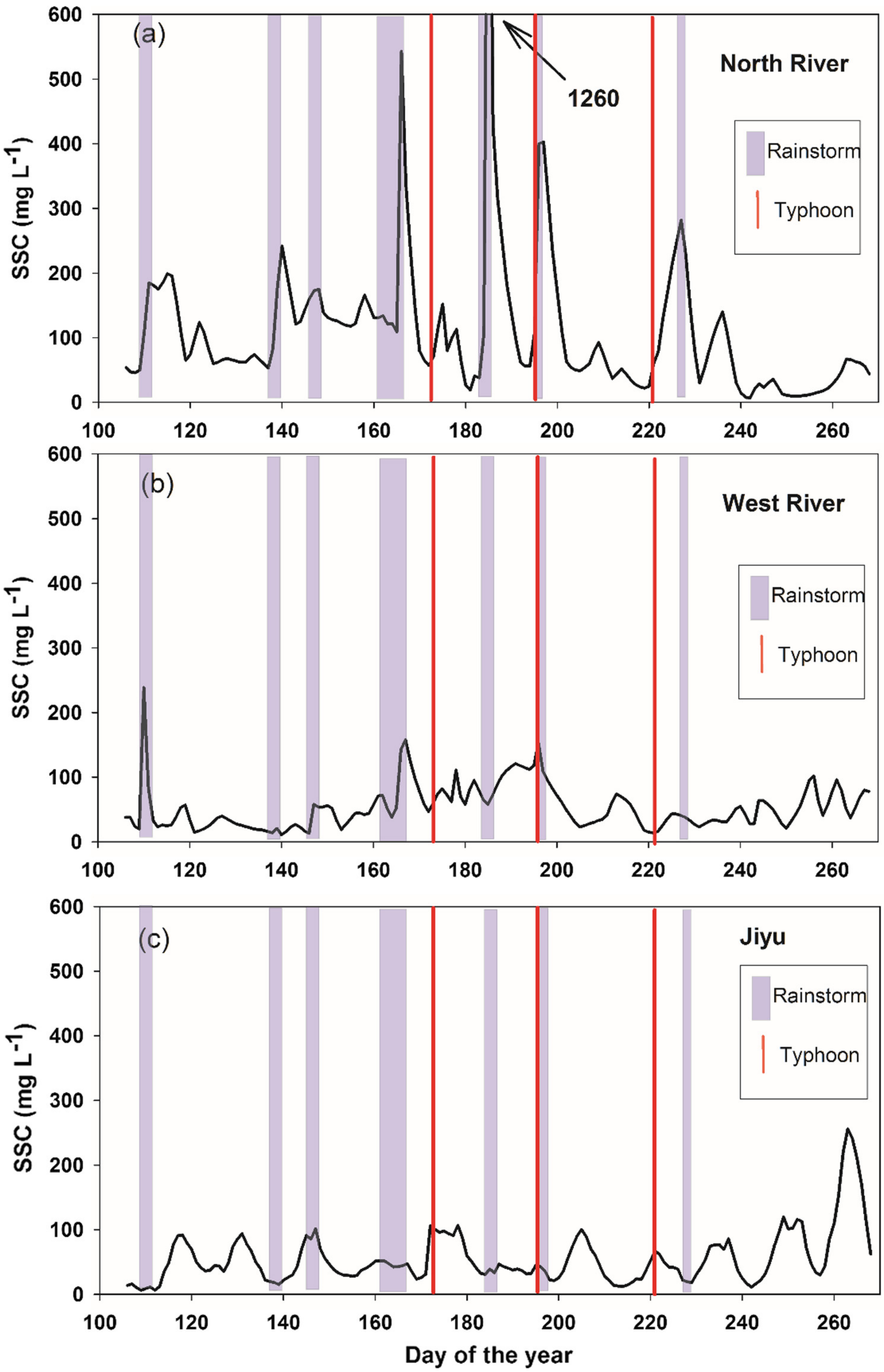

Fig. 8. The time series of SSC data throughout 16th April to 25th September 2009 of the (a) North River (Punan), (b) the West River (Zhengdian), and (c) the tidal-filtered SSC obtained from the buoy at Jiyu Island. An extreme value of 1260 mg L^{-1} of the North River was excluded from the top panel. The records of rain storms (the meteorological definition of a rain storm is the daily rainfall greater than 50 mm) and typhoons were sourced from the 2009 Climate Bulletin of Fujian Province.

hydropower stations currently in use are privately-owned (personal communication with the local Hydraulic Bureau). In the West River, those small hydropower stations in the upper stream area do not flush out sediment trapped in their reservoirs for economical reasons, resulting in considerable sediment retention and consequent decrease (82%) in sediment delivery to the estuary. In contrast, the North River, where most of the major hydropower stations are located, has been maintained regular operations of hydraulic flushes during flood seasons. As a consequent, there is only a slight decrease (11%) in sediment discharge after 1995.

In a study on the long term river sediment transport pattern in the Red River watershed (Vietnam), Dang et al. (2010) also identified a similar change of sediment – flow discharge linearity to our results. In their study, the linearity between the annual sediment discharge and the annual flow discharge decreased after dam-reservoir disturbance. The accumulative curve of the Jiulong River

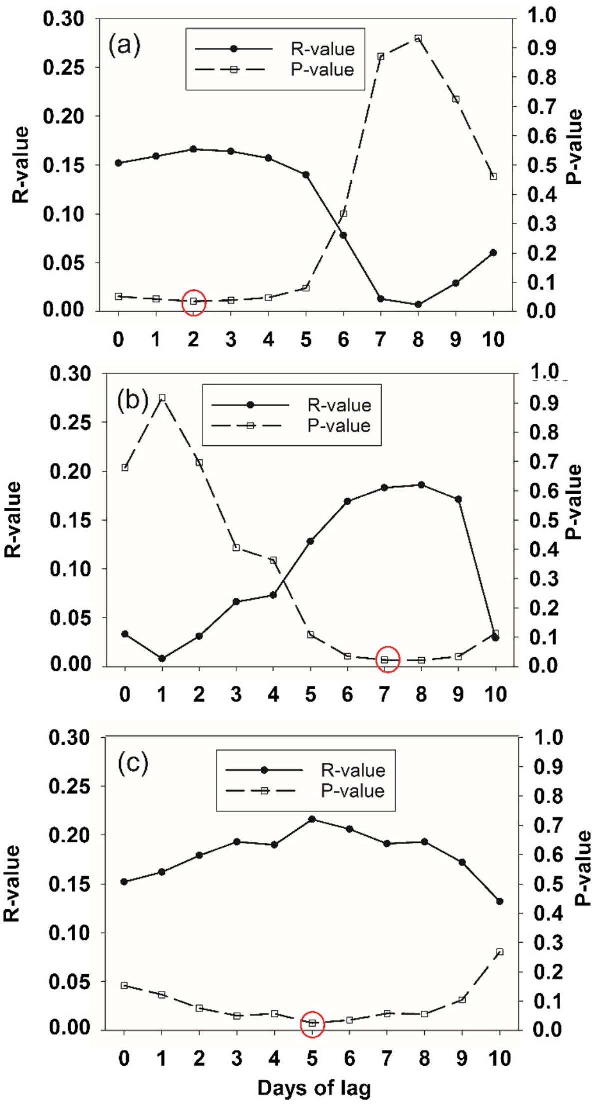

Fig. 9. The results of linear regression tests for the SSC data between the river stations (PN, ZD) and the estuary station (JY) throughout a wet season: (a) linear regression between the North River SSC and the Jiyu SSC; (b) linear regression between the West River SSC and the Jiyu SSC; and (c) multiple linear regression between the North River SSC, West River SSC and the Jiyu SSC. R is the correlation coefficient and P is the probability for the null-hypothesis test.

(Fig. 3) also shows a similar decrease in the slope as the Yangtze River, which has been attributed to the construction of large dam reservoirs (Wang et al., 2008). However, unlike previous studies, this anthropogenic effect on the sediment transport of the Jiulong River is more pronounced with high density but small dam reservoirs.

Based on the discussion above, we conclude that the long-term variation of sediment yield in the West River (82% reduction) and the North River (11% reduction) is most likely to be caused by dams and reservoirs, and is consistent with the global trend (Wang et al., 2015; Vörösmarty et al., 2003; Walling and Fang, 2003).

4.2. Sediment transport across maximum turbidity zone: Response of the estuary to river input

The primary factor affecting the sediment discharge from the river to the estuary has been identified in this study, but how the sediment discharge causes changes in the estuary over multiple timescales remains unsolved. Mass balance concepts and continuity equations have long been adopted for coastal studies, and in particular, box model studies (Knudsen, 1900). In our study, water mass conservation is considered as well as sediment mass conservation. Thus, the momentum balance can be ignored. Assuming a steady balance, a simplified box model was set up between the river reach and the estuary (Fig. 10), to consider the response of the estuary to the river sediment input at different timescales. It should be noted that the processes (e.g. flocculation) occurring within an estuarine maximum turbidity zone can be highly complex (Brenon and Hir, 1999; Uncles and Stephens, 1993), and so the box model represents a highly simplified scenario. The west boundary of the box model is located at site A3 (Fig. 1), where the North River meets the West River, and the east boundary of the box is at Jiyu Island.

The river input from the North River and West River, and the seawater pumped in by tides are considered to be the main factors controlling the model. Evaporation, water mass loss along the transport pathway and the addition from the other small tributary – the South River – are neglected for simplicity. Q_r, S_r, and C_r are defined as the flow discharge, salinity and suspended sediment concentration of the river input. Q_i, S_i, and C_r are the same variables for the sea input by tides. Q_0, S_0, and C_0 are the net output variables of the estuary. F_c is the sediment trapped in this system, which can be roughly estimated by the total area of the estuary seabed A and the sedimentation rate R.

The water mass balance gives:

$$Q_r + Q_i = Q_0 \quad (4)$$

The salinity balance gives:

$$Q_rS_r + Q_iS_i = Q_0S_0 \quad (5)$$

As the salinity of the river flows, S_r, is zero, then

$$Q_0 = \frac{S_i}{S_i - S_0}Q_r \quad (6)$$

$$Q_i = \frac{S_0}{S_i - S_0}Q_r \quad (7)$$

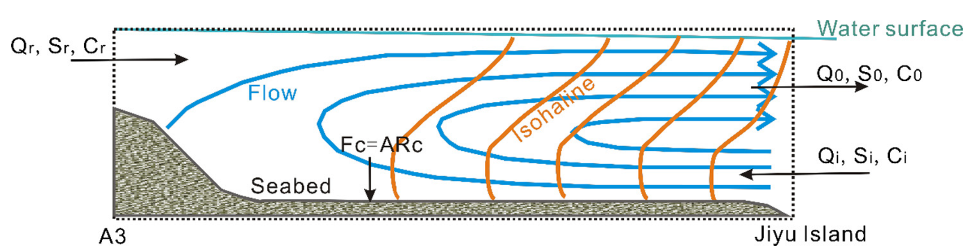

Fig. 10. The schematic graph of estuarine mixing model of Jiulong Jiang Estuary, including the riverine input (Q_r = river flow discharge, S_r = river flow salinity, C_r = sediment concentration of river input), the riverine output (Q_0 = flow discharge to the sea, S_0 = salinity of flow to the sea, C_0 = sediment concentration of flow to the sea), the tidal input (Q_i = flow discharge of tidal input, S_i = salinity of tidal input, C_i = sediment concentration of tidal input) and the sedimentation of the seabed (Fc). The gray line marks the front between fresh water and salt water, which varies with mixing conditions. The A3 is where the North River meets the West River, which is used as the upper stream boundary of the box model.

The mass balance of sediments gives:

$$Q_rC_r + Q_iC_i = Q_0C_0 + F_c \quad (8)$$

Replace the items of Eq. (8) with Eqs. (6) and (7) to get:

$$C_r = \frac{S_iC_0 - S_0C_i}{S_i - S_0} + \frac{F_c}{Q_r} \quad (9)$$

Eq. (9) can be further written as:

$$\frac{C_r}{C_i} = \frac{S_iC_0 - S_0C_i}{C_i(S_i - S_o)} + \frac{F_c}{Q_rC_i} \quad (10)$$

Eq. (10) can be reorganized as:

$$\frac{C_r}{C_i} = 1 - \frac{\frac{C_i - C_0}{C_i}}{\frac{S_i - S_0}{S_i}} + \frac{F_c}{Q_rC_r}\frac{C_r}{C_i} \quad (10')$$

$$\frac{C_r}{C_i} = \frac{1 - \frac{\frac{C_i - C_0}{C_i}}{\frac{S_i - S_0}{S_i}}}{1 - \frac{F_c}{Q_rC_r}} \quad (10'')$$

$$\frac{C_r}{C_i} = \frac{1 - \frac{\text{SSC stratification}}{\text{Salininty stratification}}}{1 - \frac{\textit{Sediment trapping by estuary}}{\textit{River sediment input}}} \quad (10''')$$

Similarly, we get:

$$\frac{C_r}{C_0} = 1 - \frac{\frac{C_i - C_0}{C_0}}{\frac{S_i - S_0}{S_0}} + \frac{F_c}{Q_rC_0} \quad (11)$$

$$\frac{C_r}{C_0} = \frac{1 - \frac{\text{SSC vertical change}}{\text{Salininty vertical change}}}{1 - \frac{\textit{Sediment trapping by estuary}}{\textit{River sediment input}}} \quad (11')$$

Eqs. (11) and (11′) describes the response of the estuary to the river input over multiple timescales. The suspended sediment response behavior is determined by the sediment trapping/passing rate within the estuary and the vertical structure of suspended sediments salinity at the seaward boundary of the estuary. Secondly, the suspended sediment concentration at the estuary varies with river sediment input in a linear way when the sediment trapping rate keeps the same varying pace with the sediment-salinity vertical structure of the estuary. Therefore, the estuary responds to the river input sometimes in a linear way with a response lag as observed by Fig. 9.

Over a long period, the response of the estuary to river inputs from the North River and West River can be compared, because the estuarine end condition and the average sediment trapping rate can be considered to be the same. Under those conditions, greater river sediment input will increase the suspended sediment in the estuary. Before 1995, the West River contributed more sediment input to the Jiulong River and thus the estuary condition was mainly a response to the West River input. After 1995, the North River input became more important in affecting the suspended sediment concentration in the estuary.

In order to test the long-term response of the estuary to the river input, the river input before and after 1995 was regarded as the main variable for the box model to test. The data of the salinity and the SSC under the partially mixed condition of the estuary ($S_i = 25$, $S_0 = 15$, $C_i = 100\ \text{mg L}^{-1}$, $C_0 = 10\ \text{mg L}^{-1}$) (Wang et al., 2013) were used to estimate the change of F_c before and after 1995. The calculation based on Eq. (6) showed that before 1995, the total amount of sediment trapped annually within the area between the two hydrological stations and the outer boundary of the estuary (Jiyu) was 7.4×10^6 tons including 5.9×10^6 tons of sediments from river input. However, after 1995, the total amount of sediment trapped by the estuary decreased to 5.1×10^6 tons, including 3.6×10^6 tons from the river. Thus, the percentage of marine sediments increased from 20% to 30% after 1995.

At the seasonal scale, Eq. (11) should be considered under separate dry season and wet season scenarios. During the dry season the estuary is well mixed and the vertical change of salinity is very limited, whilst the vertical change of SSC could be considerable due to the resuspension of sediments near the sea bed. Therefore, the vertical structure term could be much greater than the sediment trapping rate term, resulting in a minor response of the estuary. During wet seasons, the response of the estuary to the river input is determined by both the sediment trapping term and the vertical structure term, and the paces between those two terms can cause a delayed response of the estuary. Under this scenario, the river sediment input quantity is less important, but the pace-match is regulating the response of the estuary. As such, a delayed response is expected, as revealed by the regression analysis on the synchronous data in the wet season of 2009 (Section 3.5).

At short timescales, rainstorm events are the primary factor affecting sediment transport from the river to the estuary (Section 3.5), and cause the estuary to become stratified. Guo and Jiang (2010) used a ROMS model to simulate suspended sediment transport during a rainstorm (river input flow discharge = 1600 $\text{m}^3\ \text{s}^{-1}$) and found the suspended sediment concentration showed a reduction from the surface to the seabed ($S_i = 28$, $S_0 = 8$, $C_i = 120\ \text{mg L}^{-1}$, $C_0 = 100\ \text{mg L}^{-1}$, $C_r = 460\ \text{mg L}^{-1}$). The estimated sedimentation rate was 17.1 cm yr^{-1}, which is significantly higher than the long-term sedimentation rate observed (2.6 cm yr^{-1}) (Liu et al., 2012). During rainstorm periods the estuary mainly serves as a trap to the river input. Due to the large input of fresh water, the total exchange flow is inhibited and pushed seaward. Thus, a large amount of sediment has to settle down before reaching the estuary and this might cause the delayed suspended sediment response in the estuary (Fig. 9).

Previous studies on other river-estuary systems with dam construction have revealed that the primary influences of river input on the estuary can be classified into two types: (1) salt wedge dynamic changes in the estuary, for example, hydropower stations on the Ebro River in Spain have been found to increase the salt wedge frequency during middle flow discharge conditions (Ibàñez et al., 2015); and (2) channel scours in the lower estuary, such as the Trinity River in the USA (Phillips et al., 2005). These two folders of influences have been both included into our model (Eq. (11′)) in a simple way using the SSC as a tracer, and these consequences are eventually the responses of the estuary to the river suspended sediment input.

5. Conclusions

We combined long-term flow discharge and sediment discharge from the Jiulong River with measured SSC data at its estuary during a wet season to investigate the flow-sediment relationship and response of the estuary to the river input at multiple timescales. Based on time series analyses and box model estimates, the primary findings are summarized as follows:

(1) A remarkable change in 1995 was revealed by the long-term data, in terms of the flow and sediment transport by those two rivers. Before 1995, the North River was the primary convey for flow discharge whilst the West River delivered more sediment. After 1995, however, the sediment discharge by the West River decreased considerably and the North River became the main path for flow and sediment delivery.

(2) The annual flow discharge and sediment discharge data showed a linear relationship for the North River throughout 1967–2014, whilst the flow-sediment relationship of the West River switched from non-linear to linear after 1995. The most likely reason for this change was the construction of small dams and reservoirs in the West River after 1995.
(3) The synchronous SSC data of the river SSC input and the estuary SSC data were analyzed by a regression model, which revealed a delayed response of 5 days in the estuary to the river input. In addition, rainstorm events have a pronounced influence on rivers.
(4) A box model was established to quantitatively describe the response of the estuary to the river input over multiple timescales. The model revealed that over a long time period, the magnitude of river input determines the output of the estuary. Overall, the reduction of riverine sediment yield increased marine sediments trapped into the estuary. Over shorter time scales, the relative changes of vertical SSC and salinity, together with the sediment trapping rate, control the sediment response of the estuary.

Acknowledgments

This research was supported by the National Natural Science Foundation of China [grant numbers 41376082, 41676098, 41576095], Fujian Natural Science Foundation of China [grant number 2016J01197], and the Fundamental Research Funds for the Central Universities [grant number 20720160120]. We thank the crew on R/V Ocean II and R/V Yanping II for their assistance in the cruises. Special thanks are given to Hydrological Stations for providing flow and sediment data and to Oceans and Fisheries Bureau of Xiamen for providing buoy data. We also would like to take this opportunity to thank the anonymous reviewers for their thoughtful comments.

References

Brenon, I., Hir, P.L., 1999. Modelling the turbidity maximum in the seine estuary (France): identification of formation processes. Estuar. Coast. Shelf Sci. 49 (4), 525–544.
Cai, F., Huang, M.F., Su, X.Z., Zhang, H.F., 1999. Characteristics of silt movement and sedimentary dynamic mechanism in Jiulongjiang Estuary. J. Oceanogr. Taiwan Strait 18 (4), 418–424 (In Chinese with English abstract).
Chen, X., 2007. Assessment and management of rainstorm-flood hazard risk in Fujian province. J. Water Soil Convers. 14, 180–185 (In Chinese with English Abstract).
Dai, S.B., Yang, S.L., Cai, A.M., 2008. Impacts of dams on the sediment flux of the Pearl River, southern China. Catena 76 (1), 36–43.
Dai, S.B., Yang, S.L., M, L.I., 2009. The sharp decrease in suspended sediment supply from China's rivers to the sea: anthropogenic and natural causes. Hydrol. Sci. J. 54 (1), 135–146.
Dang, T.H. et al., 2010. Long-term monitoring (1960–2008) of the river-sediment transport in the Red River Watershed (Vietnam): temporal variability and dam-reservoir impact. Sci. Total Environ. 408 (20), 4654.
David, F., Martin, S., Alfred, W., 2006. Effects of upstream hydropower operation on riverine particle transport and turbidity in downstream lakes. Water Resour. Res. 42 (8), 375–387.
Dearing, J.A., Jones, R.T., 2003. Coupling temporal and spatial dimensions of global sediment flux through lake and marine sediment records. Global Planet. Change 39 (1–2), 147–168.
Dyer, K.R., Christie, M.C., Manning, A.J., 2004. The effects of suspended sediment on turbulence within an estuarine turbidity maximum. Estuar. Coast. Shelf Sci. 59 (2), 237–248.
Finger, D., Schimd, M., Wüest, A., 2006. Effects of upstream hydropower operation on riverine particle transport and turbidity in downstream lakes. Water Resour. Res. 42, W08429. https://doi.org/10.1029/2005WR004751.
Garcíaruiz, J.M., 2010. The effects of land uses on soil erosion in Spain: a review. Catena 81 (1), 1–11.
Guo, M., Jiang, Y.W., 2010. Distribution of suspended sediment and erosion simulation of the Jiulong River Estuary during a flood process. J. Xiamen Univ. (Nat. Sci.) 49 (5), 688–692 (in Chinese).
Huang Jr, J., R.G.P., Li, Q., Zhang, Y., 2012. Use of intensity analysis to link patterns with processes of land change from 1986 to 2007 in a coastal watershed of southeast China. Appl. Geogr. 34 (3), 371–384.
Huang, J., Li Jr, Q., R.G.P., Klemas, V., Hong, H., 2013. Detecting the dynamic linkage between landscape characteristics and water quality in a subtropical coastal watershed, Southeast China. Environ. Manage. 51 (1), 32.
Huang, J.L., Hong, H.S., Zhang, L.P., 2004. Study on predicting soil erosion in jiulong river watershed based on GIS and USLE. J. Soil Water Conserv. 18 (5), 75–79 (In Chinese with English abstract).
Huang, X., 2008. The hydrology of Jiulong River watershed. Hydraulic Sci. Technol. 1, 16–20 (In Chinese).
Ibàñez, C., Prat, N., Canicio, A., 2015. Changes in the hydrology and sediment transport produced by large dams on the lower Ebro river and its estuary. River Res. Appl. 12 (1), 51–62.
Ji, D., 2006. Study for the three-dimensional tidal current numerical model in Xiamen Bay. Xiamen University, p. 90.
Jiang, H., Wang, X., Chen, Y., 2007. Remote sensing monitoring and analysis on soil erosion changes of Jiulong River watershed. In: Proceedings of annual meeting of Fujian Province Land Society, Fuzhou, China, p.6 (In Chinese).
Jiang, X.Y., Zhi-Zhong, L.I., Jin-Quan, L.I., Kong, X.G., Guo, Y., 2012. Stalagmite δ~(18) O record from Yuhua cave over the past 500 years and its regional climate significance. Sci. Geogr. Sin. 32 (2), 207–212 (In Chinese with English abstract).
Jiang, Y.W., Wai, O.W.H., 2005. Drying–wetting approach for 3D finite element sigma coordinate model for estuaries with large tidal flats. Adv. Water Resour. 28 (8), 779–792.
Kao, S.J., Lee, T.Y., Milliman, J.D., 2005. Calculating highly fluctuated suspended sediment fluxes from mountainous rivers in Taiwan. Terr. Atmos. Oceanic Sci. 16 (3), 653–675.
Khoi, D.N., Suetsugi, T., 2012. The responses of hydrological processes and sediment yield to land-use and climate change in the Be River Catchment, Vietnam. Hydrol. Process. 28 (3), 640–652.
Knudsen, M., 1900. Ein hydrographischer Lehrsatz. Ann. Hydrogr. Maritimen Meteorol. 28, 316–320.
Lane, S.N., Tayefi, V., Reid, S.C., Yu, D., Hardy, R.J., 2007. Interactions between sediment delivery, channel change, climate change and flood risk in a temperate upland environment. Earth Surf. Proc. Land. 32 (3), 429–446.
Li, P. et al., 2012. Spatial, temporal, and human-induced variations in suspended sediment concentration in the surface waters of the Yangtze estuary and adjacent coastal areas. Estuaries Coasts 35 (5), 1316–1327.
Lin, Y.H., Pan, W.R., Zhang, G.R., Ma, T., 2009. The numerical simulation of wind wave in Xiamen Bay. J. Xiamen Univ. (Nat. Sci.) 48, 298–301 (In Chinese with English abstract).
Lin, Y.L., Ensley, D.B., Chiao, S., Huang, C.Y., 2002. Orographic influences on rainfall and track deflection associated with the passage of a tropical cyclone. Mon. Weather Rev. 130 (12), 2929–2950.
Liu, J.P. et al., 2008. Flux and fate of small mountainous rivers derived sediments into the Taiwan Strait. Mar. Geol. 256 (1), 65–76.
Liu, Z. et al., 2012. Sediment distribution and deposition rate in the Xiamen Bay and adjoining waters. Mar. Sci. 36 (6), 1–8 (In Chinese).
Meade, R.H., 1996. River-sediment inputs to major deltas. In: Milliman, J.D., Haq, B. U. (Eds.), Sea-level rise and Coastal Subsidence: Causes Consequences and Strategies. Kluwer Academic Publishers, Dordrecht, pp. 63–85.
Meade, R.H., Moody, J.A., 2010. Causes for the decline of suspended-sediment discharge in the Mississippi River system, 1940–2007. Hydrol. Process. 24 (1), 35–49.
Meybeck, M., 1988. How to establish and use world budgets of riverine materials. In: A. Lerman., M. Meybeck.A. Lerman., M. Meybeck. (Ed.), Physical and Chemical Weathering in Geochemical Cycles. NATO ASI Series (Series C: Mathematical and Physical Sciences). Springer, Dordrecht.
Milliman, J.D., Farnsworth, K.L., 2011. River Discharge to the Coastal Ocean – A Global Synthesis. Cambridge University Press, Cambridge, UK.
Milliman, J.D., Kao, S.J., 2005. Hyperpycnal discharge of fluvial sediment to the ocean: impact of auper-yyphoon herb (1996) on Taiwanese rivers. J. Geol. 113 (5), 503–516.
Milliman, J.D. et al., 2007. Short-term changes in seafloor character due to flood-derived hyperpycnal discharge: typhoon Mindulle, Taiwan, July 2004. Geology 35 (9), 779–782.
Milliman, J.D., Meade, R.H., 1983. World-wide delivery of river sediment to the oceans. J. Geol. 91 (1), 1–21.
Milliman, J.D., Syvitski, J.P.M., 1992. Geomorphic/tectonic control of sediment discharge to the ocean: the importance of small mountainous rivers. J. Geol. 100 (5), 525–544.
Phillips, J.D., Slattery, M.C., Musselman, Z.A., 2005. Channel adjustments of the lower Trinity River, Texas, downstream of Livingston Dam. Earth Surf. Proc. Land. 30 (11), 1419–1439.
Syvitski, J.P.M., Kettner, A.J., Peckham, S.D., Kao, S.-J., 2005. Predicting the flux of sediment to the coastal zone: application to the Lanyang watershed, Northern Taiwan. J. Coastal Res. 213, 580–587. https://doi.org/10.2112/04-702a.1.
Syvitski, J.P.M., Saito, Y., 2007. Morphodynamics of deltas under the influence of humans. Global Planet. Change 57 (3–4), 261–282.
Takahashi, M., Nakamura, F., 2011. Impacts of dam-regulated flows on channel morphology and riparian vegetation: a longitudinal analysis of Satsunai River, Japan. Landscape Ecol. Eng. 7 (1), 65–77.
Tucker, M., 1988. Techniques in Sedimentology. Blackwell Scientific Publications.

Uncles, R.J., Stephens, J.A., 1993. The freshwater-saltwater interface and its relationship to the turbidity maximum in the Tamar Estuary, United Kingdom. Estuaries 16 (1), 126–141.

Vörösmarty, C.J. et al., 2003. Anthropogenic sediment retention: major global impact from registered river impoundments. Global Planet. Change 39 (1), 169–190.

Wall, G.R., Nystrom, E.A., Litten, S., 2008. Suspended sediment transport in the freshwater reach of the hudson river estuary in eastern New York. Estuaries Coasts 31 (3), 542–553.

Walling, D.E., 1983. The sediment delivery problem. J. Hydrol. 65 (1), 209–237.

Walling, D.E., Fang, D., 2003. Recent trends in the suspended sediment loads of the world's rivers. Global Planet. Change 39 (1), 111–126.

Wang, G. et al., 2010. Valuing the effects of hydropower development on watershed ecosystem services: case studies in the Jiulong River Watershed, Fujian Province, China. Estuar. Coast. Shelf Sci. 86 (3), 363–368. doi: 10.1016/j.ecss.2009.03.022.

Wang, H., Yang, Z., Wang, Y., Saito, Y., Liu, J.P., 2008. Reconstruction of sediment flux from the Changjiang (Yangtze River) to the sea since the 1860s. J. Hydrol. 349 (3–4), 318–332.

Wang, J., 2013. Research on the dynamics and mass flux in Xiamen Bay. Xiamen University, p. 62 (In Chinese with English abstract).

Wang, S. et al., 2015. Reduced sediment transport in the Yellow River due to anthropogenic changes. Nat. Geosci. 9 (1).

Wang, Y.L., Chen, J., Zeng, Z., Zhao, G.T., Liao, K.M., 2005. Distribution and diffusion of water body with high suspended sediment concentration in Jiulongjiang Estuary. J. Oceanogr. Taiwan Strait 24 (3), 383–393 (In Chinese with English abstract).

Wang, Y.P. et al., 2013. Sediment resuspension, flocculation, and settling in a macrotidal estuary. J. Geophys. Res. Oceans 118 (10), 5591–5608.

Woods, R., 2003. The relative roles of climate, soil, vegetation and topography in determining seasonal and long-term catchment dynamics. Adv. Water Resour. 26, 295–306. https://doi.org/10.1016/S0309-1708(02)00164-1.

Xu, J., Hong, J., 2000. Activity regularity analysis of typhoon landing in south Fujian. J. Oceanogr. Taiwan Strait 19 (3), 293–298 (In Chinese with English abstract).

Ye, Q., Huang, M., 2009. Evolution and prospect of adjustment of agriculture structure in Fujian from reform and opening. Taiwan Agric. Res. 2, 44–50.

Zhang, Z., Huang, J., Huang, Y., Hong, H., 2015. Streamflow variability response to climate change and cascade dams development in a coastal China watershed. Estuar. Coast. Shelf Sci. 166, 209–217.

Zhu, J., 2008. The influence of the hydropower station construction within the North River on the dry season flows of the downstream, Jiulong River, the 8th Annual Conference on Hydraulics of Science Society of Fujian Province, Putian, pp. 38–41. (In Chinese)